Journal of Materials Science: Materials in Electronics (2018) 29:6530–6542
https://doi.org/10.1007/s10854-018-8635-x

Photocatalytic activity and photoluminescence properties of TiO_2, In_2O_3, TiO_2/In_2O_3 thin films multilayer

L. M. P. Garcia[1] · M. T. S. Tavares[2] · N. F. Andrade Neto[1] · R. M. Nascimento[1] · C. A. Paskocimas[1] · E. Longo[3] · M. R. D. Bomio[1] · F. V. Motta[1]

Received: 28 November 2017 / Accepted: 18 January 2018 / Published online: 20 January 2018

Abstract
This study evaluated the effect of crystallization temperature (300, 500 and 700 °C) on the photocatalytic and photoluminescent properties of the multilayer thin films of TiO_2, In_2O_3 and TiO_2/In_2O_3 which were prepared by the Complex Polymerization Method (CPM) and deposited on substrates of Si (100) by the spin coating method. The results of X-ray diffraction (XRD) revealed that there was no chemical interaction between the oxides (TiO_2/In_2O_3) in crystalline films. The morphology was observed by atomic force microscopy (AFM) with a mean grain size of 15–35 nm. The result showed that the photocatalytic property is significantly increased by increasing the crystallization temperature. This is due to the agitation of the molecules which facilitates the transfer of charge between the electron and the catalyst bore. UV–vis light absorption spectra indicated that the addition of In_2O_3 in TiO_2 films is an effective way of increasing the uptake of TiO_2 in the visible region up to ~600 nm for photocatalytic applications, it was also possible to observe that these films could be easily Recycled for reuse. The samples were also characterized by photoluminescence, where it was possible to observe that the reduction of the PL intensity increased the photocatalytic activity of the thin films, with the increase of the crystallization temperature. In addition, the method used in this study is simple and economical compared to other methods.

1 Introduction

Constant studies in the production of thin films and nanocomposites have grown considerably in the last decade, given that their properties have a strong scientific and technological appeal due to their wide range of applications such as photocatalysts [1–3], solar cells [4], pigments [5, 6], medical diagnostics [7], humidity sensors [8], among others. TiO_2/In_2O_3 composite thin have been used in solar cells, in order to improve the electrical properties of TiO_2 and increase the efficiency of the photovoltaic energy conversion [9, 10].

Among the diffused methods for processing thin films, such as sputtering [11], atomic layer deposition (ALD) [12], spray pyrolysis [13], sol–gel [14], we chose the Complex Polymerization Method. The method of polymerization of complexes is a simple and economical method, this method uses the polymerization in situ, that is, it occurs inside the reaction vessel itself. The term polymeric precursors come from the synthesis of an organic polymer, followed by solubilization of the metal cations. The difference between methods, MP and MPC, is in the way the resin is prepared. In the MPC, soluble metal coordination compounds with citric acid (AC) are prepared, and only then is the polyalcohol, in this case ethylene glycol (EG), which promotes the polymerization of the metal complexes [15]. The selection of the precursor and the solvent, the molarity of the solution, the preheating process and the final annealing are the important parameters that influence the quality of the obtained films.

Titanium dioxide (TiO_2) is the most studied photocatalytic material, having high chemical stability and non-toxic properties. Unfortunately, this material has a wide band gap (anatase, 3.2 eV, rutile, 3.0 eV), so that its absorption usually occurs below 400 nm [16]. More recently, differents metals and metal cations, like Ag, In, Sb, Fe^{3+}, Mo^{5+}, Ru^{3+},

✉ L. M. P. Garcia
lauengmat@hotmail.com

[1] Department of Science and Engineering Materials, Universidade Federal do Rio Grande do Norte, Natal, RN 59072-970, Brazil

[2] Instituto Federal da Bahia, Campus Feira de Santana, Feira de Santana, BA 44096-486, Brazil

[3] Chemistry Institute, University of the State of São Paulo Julio de Mesquita Filho-UNESP, Francisco Degni, Araraquara, SP 14800-900, Brazil

Os^{3+}, Re^{5+}, V^{4+}, Rh^{3+} and non-metallic anions N, C, S, B, P, F have been doped into TiO_2 to increase the visible light absorption, which enhanced the photocatalytic activity and exceptional characteristics compared with the pure TiO_2 [3, 16]. The photocatalytic property of TiO_2 is influenced by many factors, such as crystalline structures, particle size, doping elements and surface area, i.e. due to its quantization effect and to its large specific surface area [17].

Indium based oxides have attracted an increasing attention in the last few years because of their properties of potential value in optoelectronic devices, biological applications, catalysis and other technologies [18]. The power of the indirect band In_2O_3 is 2.8 eV and the conduction band is more negative than the potential of self-corrosion of metals. Thus, the thin film of indium oxide can be a photo anode potential for corrosion protection under irradiation of visible light [19].

Many efforts have been made to the further improvement of TiO_2 photocatalytic performance for degradation of various organic pollutants, one of the ways is the preparation of multilayer thin films with other semiconductors [20]. The combination of TiO_2/In_2O_3 allows to transfer the photogenerated electrons from the surface to the In_2O_3 for TiO_2 conduction band. This process results in the effective capture of photogenerated electrons and a delayed recombination of photogenerated electron–hole pairs. Recent studies have shown that the photocatalytic activity of TiO_2/In_2O_3 films exceeds the individual In_2O_3 and TiO_2 [3, 10].

Recently, some authors have reported structural and optical investigations on thin films, but one of the main advantages of our work is the simplicity of preparation of the complex polymerization method. In this study, thin films of TiO_2, In_2O_3 and TiO_2/In_2O_3 multilayers were deposited using the spin coating method, the use of multilayers was aimed at increasing the number of accessible surface active sites and improving light scattering, leading to increased photocatalytic activity. The photocatalytic properties of thin films were investigated based on the degradation of the methylene blue dye under UV irradiation.

2 Experimental

2.1 Preparation of thin films

The thin films were obtained from a precursor solution using titanium isopropoxide (IV) (Alfa Aesar) and citric acid (Synth), in a molar ratio of 3:1. The citric acid was added and dissolved in about 100 ml of destilated water under stirring at 70 °C. Then, the titanium isopropoxide was slowly added until a homogeneous and transparent solution was obtained. Finally, ethylene glycol was added to the citric acid relatively in a ratio of 40/60 (wt%) and the temperature was raised to 90 °C. The same procedure was used to obtain the resin In_2O_3, substituting titanium isopropoxide by indium (III) nitrate hydrate (Alfa Aesar). The ratio of citric acid/metal cations (titanium isopropoxide, indium nitrate) added was 3:1, while the ratio of ethylene glycol added was 40/60 (% by mass) in relation to the citric acid. The viscosity of the deposition solution was adjusted to 20 mPa/s measured at room temperature.

The silicon (100) substrates were spin-coated by dropping a small amount of the polymeric resin onto them. The rotation speed and spin time were fixed at 700 rpm for 3 s and 7200 rpm for 30 s, using a commercial spinner (Chemat Technology KW-4B spin-coater). After deposition, the wet films were dried at 80 °C for 10 min on a plate hot. Four layers were deposited for each film and the procedure was repeated for each layer. The deposition of multilayer TiO_2/In_2O_3 thin films on substrates was illustrated in Fi. 1. Finally, the films were heat-treated in a resistive furnace at 300, 500 and 700 °C for 2 h. Finding a suitable heat treatment process is vital to achieving high performance composite thin films.

2.2 Characterization measurements

The phase composition of multilayer TiO_2, In_2O_3 and TiO_2/In_2O_3 thin films was investigated in a Shimadzu/XRD-6000 diffractometer using CuKα radiation. Atomic force microscopy (AFM—Shimadzu—SPM-9700,) was used to obtain and reconstruct a 3D image of the surface of the sample. These images allow an accurate analysis and quantification of high relevant parameters such as roughness and grain size. The reflectance of the films was obtained by the UV–vis–NIR spectrophotometer (Shimadzu, UV 2600) over the spectral wavelength ranges from 200 to 1700 nm. All the measurements were taken at room temperature.

2.3 Photocatalytic activity and photoluminescent measurements

It was tested the photocatalytic properties of thin films (as a catalyst agent) for the degradation of methylene blue (MB) dye with a molecular formula [$C_{16}H_{18}ClN_3S$] (99.5% purity, Mallinckrodt) in an aqueous solution under UV-light illumination. The film was placed in a cylindrical quartz reactor, containing 3 ml of methylene blue dye solution (concentration 1×10^{-5} mol L^{-1}). The cylindrical quartz reactor was, then, placed in a photo-reactor at controlled temperature (20 °C) and, illuminated by six UVC lamps (TUV Philips, 15 W, with maximum intensity at 254 nm). In thirty-minutes intervals, the 3-mL aliquot of the dye solution was monitored and analyzed by the variations of the maximum absorption band of MB dye solutions by UV–vis absorbance spectra measurements using a Shimadzu (model UV-2600) spectrophotometer.

Photoluminescence (PL) spectra were acquired with an Ash Monospec 27 monochromator (Thermal Jarrel, U.S.A.) and a R4446 photomultiplier (Hamamatsu Photonics, U.S.A.). The 350 nm beam of a krypton ion laser (Coherent Innova 90 K) was used as the excitation source while maintaining its maximum output power at 200 mW. All measurements were performed at room temperature (Fig. 1).

3 Results and discussion

Figure 2 shows the results of XRD of the TiO_2, In_2O_3 and TiO_2/In_2O_3 films obtained by the spin-coating method and calcined at 300, 500, 700 °C. The XRD patterns of the films TiO_2 are shown in Fig. 2a. The XRD measurements show only the presence of anatase phase TiO_2 pure, indexed according to ICSDS card No. 73-1764, of which one can identify a tetragonal structure, with cell parameters of

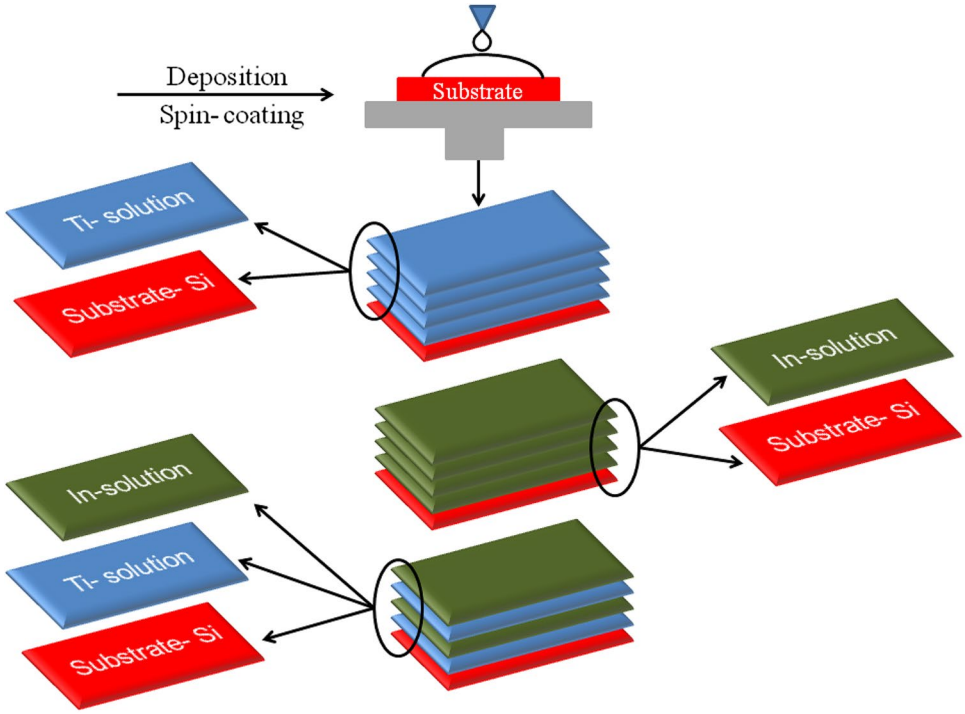

Fig. 1 Schematic representation of the process to prepare the TiO_2, In_2O_3 and TiO_2/In_2O_3 thin films

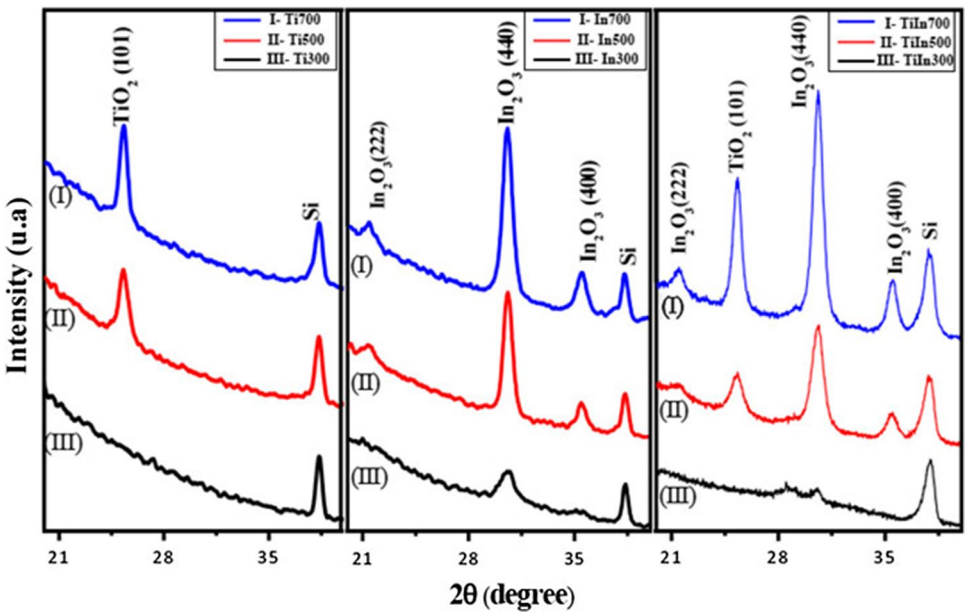

Fig. 2 X-ray diffraction of the thin films **a** TiO_2, **b** In_2O_3 and **c** TiO_2/ In_2O_3, calcined at 300, 500, and 700°C

$a = b = 3.77599$ and $c = 9.48593$ nm. The anatase structure of oxide nanocrystals is confirmed by the diffraction peak of $2\theta = 25.3°$ [21, 22].

The XRD patterns of the films In_2O_3 are shown in Fig. 2b. XRD measurements show only the presence of In_2O_3 phase in In_2O_3 pure samples. All diffraction peaks could be indexed as a cubic structure, with cell parameters of a = 10.11575 nm, which are in agreement with the respective ICSDS card No. 6-416. The In_2O_3 phase is confirmed by the diffraction peak of $2\theta = 30.3°$ [7]. In the XRD patterns of the TiO_2/In_2O_3 films (Fig. 2c), it is possible to observe well-defined peaks without overlapping phases indication and no chemical interaction between the oxides of the films. According to Poznyak [23], thin films of TiO_2/In_2O_3 prepared to different crystallization temperatures did not reveal any additional phases. Indicating that no chemical interaction occurs with TiO_2 and In_2O_3 in the range of the studied temperatures.

The average crystallite size of the thin films with anatase and In_2O_3 phases were calculated by Scherrer equation [24] using the most intense peak of each phase (101) and (440). According to Chuanhao Li [25], the width of the peak of the anatase phase increases with the formation of the TiO_2/In_2O_3 composite, indicating a reduction of crystal size according to the Scherrer equation, as can be seen in Table 1.

The morphology and particle size can influence the efficiency of materials that exhibit photocatalytic activity. Thus, by atomic force microscopy technique it was used to characterize the surface morphology, particle size and, surface roughness of pure and composite thin films, crystallized at 700 °C (Fig. 3). In the images obtained by atomic force microscopy, it was observed that the surface of the thin films is composed by rounded morphology particles and these particles are evenly distributed on the surface of the film without cracks or pores. The average particle size of the films ranged from 15 to 35 nm, which was estimated based on measurements of at least 300 microspheres in the AFM images and by fitting the resulting distribution using a Gaussian function.

The smaller particle size for the TiO_2/In_2O_3 films, compared with TiO_2 is due to the incorporation of In_2O_3, which blocks the growth of TiO_2 particles [3]. Furthermore, the variation in the particle size of all thin films synthesized was similar to the size variation calculated from the XRD patterns by Scherrer equation (Table 1).

Table 1 Average crystallite size (nm) for TiO_2, In_2O_3 and TiO_2/In_2O_3 thin films crystallized at different temperatures during 2 h

	TiO_2		In_2O_3	
	500 °C	700 °C	500 °C	700 °C
TiO_2	13.39 ± 0.573	14 ± 0.120	–	–
In_2O_3	–	–	22 ± 0.028	23 ± 0.170
TiO_2/In_2O_3	12.66 ± 0.410	14.37 ± 0.077	11.55 ± 0.212	20 ± 0.989

The average surface roughness and particle size of thin films of TiO_2, In_2O_3 and TiO_2/In_2O_3 crystallized at 500 and 700 °C are presented in Table 2. It was found that the increase of temperature promoted the increased surface roughness. A larger film roughness value increases its specific surface, facilitating the contact of the adsorbed substances with existing crystals, thereby increasing the photocatalytic efficiency [26].

The cross section of TiO_2/In_2O_3 films deposited by spin coating on silicon substrate treated at temperature of 700 °C were studied by scanning electron microscopy (SEM-FEG) and shown in Fig. 4. It is possible to observe that the thin film presents a homogeneity, thickness uniformity, adhesion to the substrate and good densification. The homogeneity and the surface thickness of the film are two main reasons that influence the optical characteristics.

As for the optical properties, the influence of the temperature on the thin films TiO_2, In_2O_3 and TiO_2/In_2O_3 in relation to the energy of the gap, and the Urbach tail were investigated. The optical band gap energy (E_{gap}) was calculated by the Kubelka and Munk method, which is based on the transformation of diffuse reflectance measurements to estimate E_{gap} values with good accuracy within the limits of the assumptions [26]. When the material is subjected to analysis by the diffuse reflectance mode, the absorption coefficient of Kubelka–Munk (K) has a value equal to 2α ($K = 2\alpha$) and the scattering coefficient (S) can be considered constant regarding the wavelength, so that the following equation is valid:

$$[F(R\infty)h\nu]^n \sim (h\nu - Eg) \quad (1)$$

where n = 2 for direct and n = 1/2 for indirect transitions.

Thus, obtaining F (R∞) by Eq. (1) and plotting a term chart $[F(R\infty)\ h\nu]^{n}$ as a function of the energy ($h\nu$), the value of the optical gap of the samples can be obtained by extrapolating the line tangent to the range in which the absorption approaches linearity in the graph [27].

According to Chen, the energy band of In_2O_3 (3,4 eV) is higher than the anatase TiO_2 (3.2 eV) [28], approximate values were obtained in this article. The Figs. 5 and 6 show the curves of the value for the indirect and direct optical band gap, respectively. It is possible to observe that there was a change in the band gap values of the films with an increase in the crystallization temperature, both for the direct band energy and for the indirect band energy. The energy band gap is controlled by the order and structural disorder, the increase in temperature causes to decrease in the structural disorder. The increased band gap energy is associated with the reduction of defects in the structural network because the lower opening band values are associated with a greater number of structural defects [28].

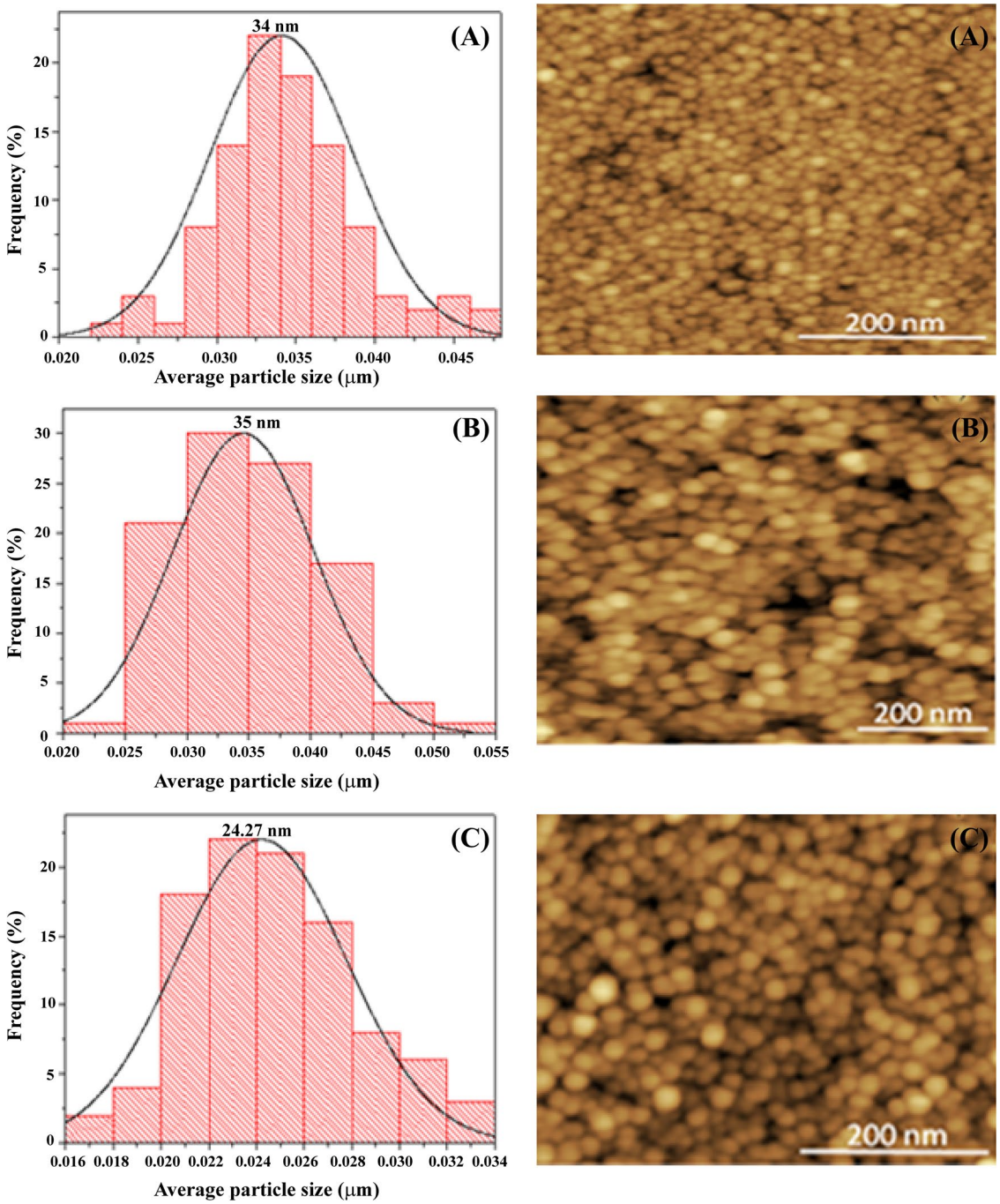

Fig. 3 Histogram distribution of particle size and image of **a** TiO_2, **b** In_2O_3 and **c** TiO_2/In_2O_3 film deposited on the surface of the (100) Si substrates with four layers and calcined at 700°C

Generally, in optical absorption, near band edges, an electron from the top of the valence band gets excited into the bottom of the conduction band across the energy band gap [29]. During this transition process, if these electrons encounter disorder, it causes density of their states ρ(hν), where hν is the photon energy, tailing into the energy gap. This tail of ρ(hν) extending into the energy band gap is termed as Urbach tail. We used a linear curve fitting to obtain the Urbach tail, which is defined as the width of the localized states available in the optical band gap that affects the optical band gap structure and optical transitions. The Urbach tail is determined by the following relation [30]:

$$\alpha = \alpha_0 \exp\left(\frac{E}{E_0}\right) \quad (2)$$

Table 2 Roughness and average particle size of the film TiO_2, In_2O_3, TiO_2/In_2O_3 calcined at 500 and 700°C

Samples	Roughness (nm)		Average size particle (nm)	
	500 °C	700 °C	500 °C	700 °C
TiO_2	–	1.74	–	34
In_2O_3	0.95	1.41	35	35
TiO_2/In_2O_3	1.43	1.48	16	24.27

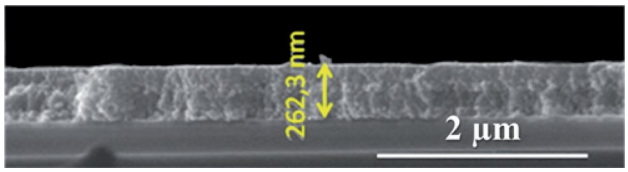

Fig. 4 Morphology of the cross section of the TiO_2/In_2O film crystallized 700°C

where α is optical absorption, E is the photon energy, (α_o) is constant and E_U is the Urbach energy, which refers to the width of the exponential absorption edge.

The value of E_U was calculated from the slope, and the obtained values are given in Table 3, which indicates that Urbach energy values for most films decrease after annealing. It can be clearly seen that the width of the band tail, i.e. the Urbach energy, decreases slightly with increasing annealing temperature, indicating an improvement of the quality of the film due to the annealing process. The E_U, values change inversely with optical band gaps of the films. This decrease leads to a redistribution of states from band to tail, thus allowing for a greater number of possible band to tail and tail transitions [31].

The photoluminescence is mainly attributed to oxygen vacancies or interstitial oxygen defects. These oxygens vacancies promote intermediate energy levels in the slot region providing a decrease in the gap band, favoring the phenomenon photoluminescence [28]. Kim et al. revealed

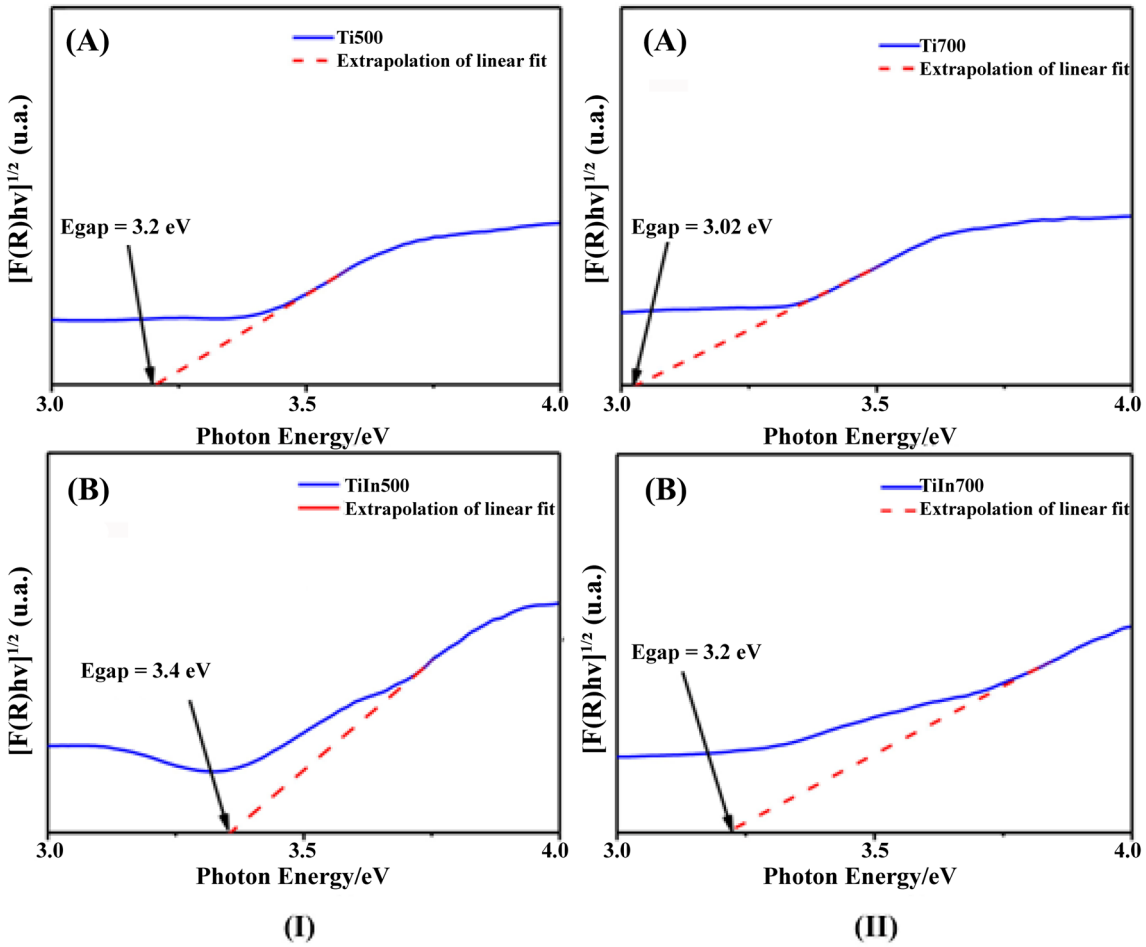

Fig. 5 UV–vis spectra of the films **a** TiO_2 and **b** TiO_2/In_2O_3 calcined at (I) 500 °C and (II) 700 °C, to obtain the indirect gap energy

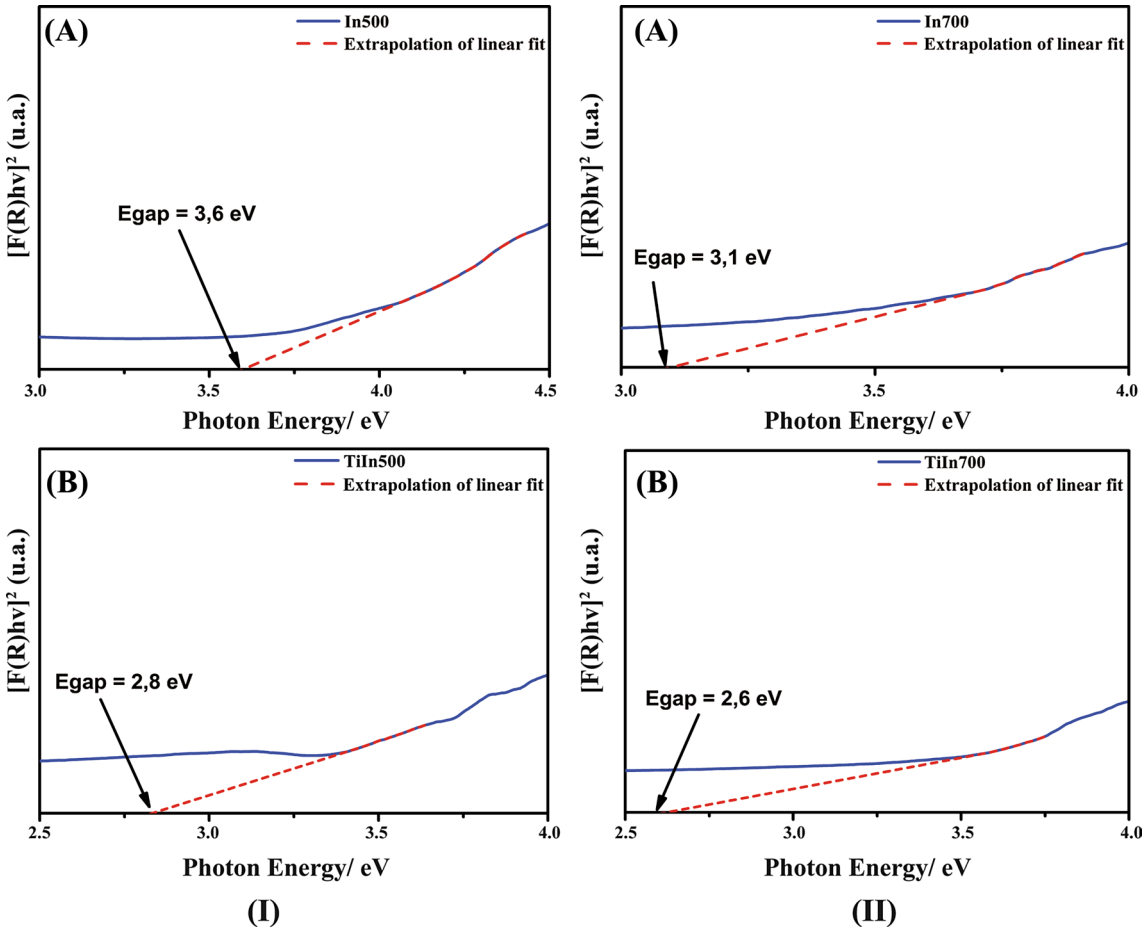

Fig. 6 UV–vis spectra of the films **a** In_2O_3 and **b** TiO_2/ In_2O_3 calcined at (I) 500 °C and (II) 700 °C, to obtain the direct gap energy

Table 3 Urbach energy values for TiO_2, In_2O_3 and TiO_2/In_2O_3 films

Samples	Urbach energy (eV)
Ti500	0.23
Ti700	0.30
In500	0.28
In700	0.41
TiIn500	0.32
TiIn700	0.29

that the PL emission from In_2O_3 nanostructures can be attributed from the recombination of electrons on singly ionized oxygen vacancies and holes on the valence band or double ionized oxygen vacancies. In particular, the In_2O_3 nanostructures with high aspect ratio will favor the generation and existence of large quantities of oxygen vacancies [32]. According to Desai the PL emission from TiO_2 can be attributed to the recombination, because in TiO_2, e^-/h^+ recombination may be grouped in two categories: (i) volume recombination—dominate in well crystalline larger size TiO2, and (ii) surface recombination—dominate in smaller size particles due to large surface area to volume ration and large number of surface active sites [33]. Figure 7 shows the photoluminescence spectra (PL) of the films (a) TiO_2, (b) In_2O_3 and (c) TiO_2/In_2O_3 calcined at 300, 500 and 700 °C. Samples were analyzed at room temperature with an excitation wavelength at 350 nm. It was possible to observe the presence of a broad band ranging from 400 to 700 nm. One may expect that introducing impurities results in change in peak intensity and positions. Inspired by this, we seek to evaluate the changes in PL spectra of thin films composed. However, since we apply thin film layers with 2 different oxides, the occurrence of complicated structural changes during fine film processing, such as removal of residual solvent and organic, hydroxyl condensation and structural relaxation is inevitable [34].

The results showed that the higher the temperature, the lower the intensity of the photoluminescence, that is, with the increase of the temperature there is an increase in the structural order. As the photoluminescence signal is the

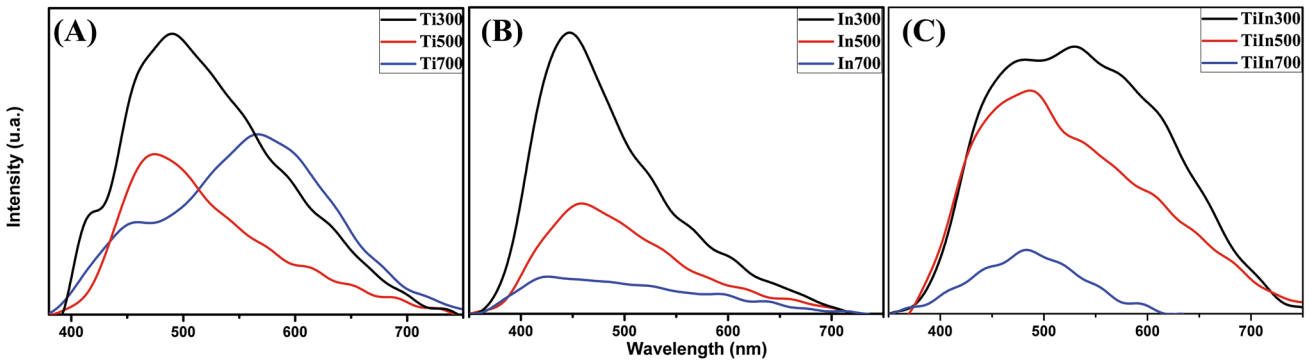

Fig. 7 PL profile of **a** TiO_2, **b** In_2O_3 and **c** TiO_2/In_2O_3 multilayered thin films as a function of annealing temperature

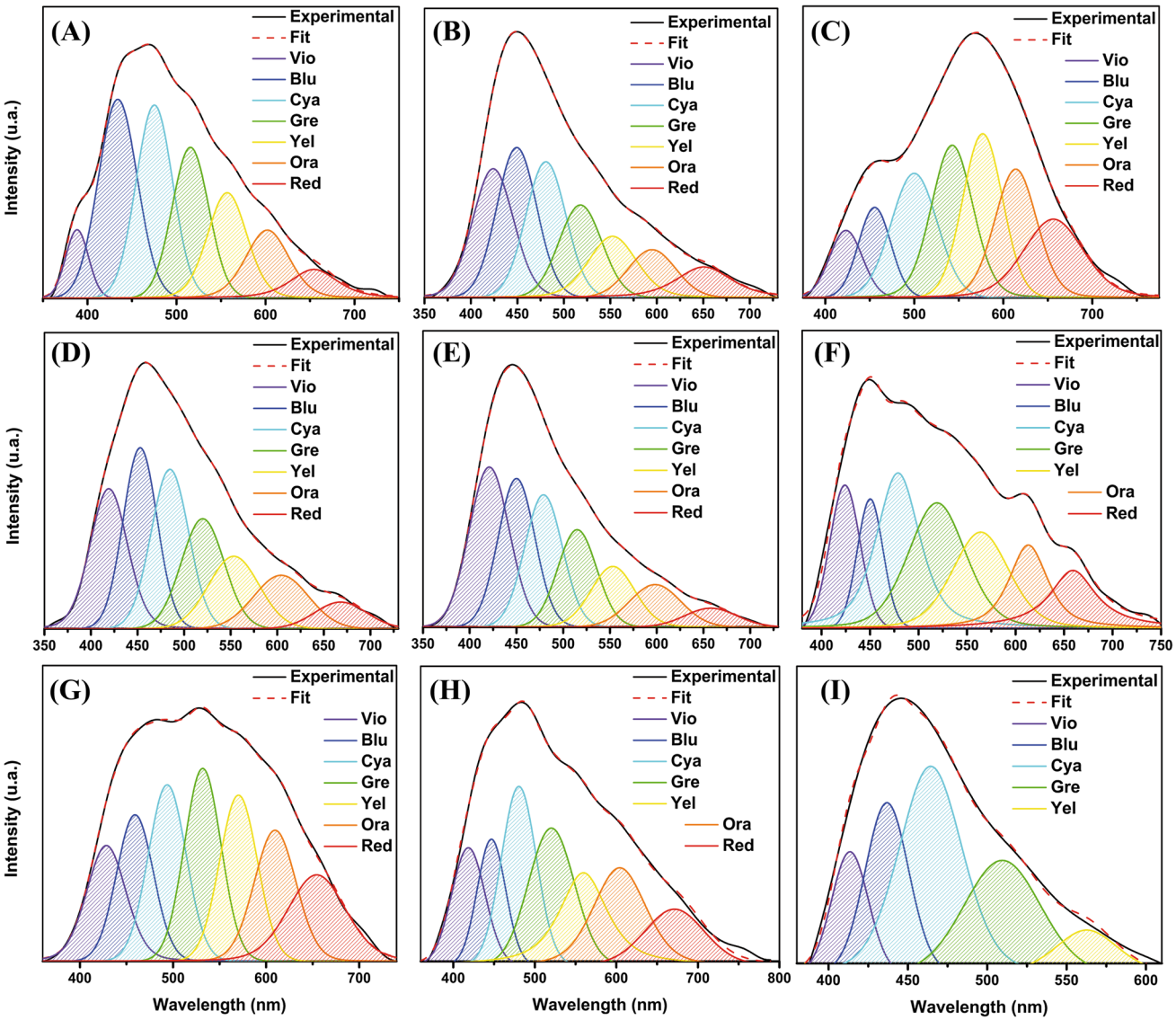

Fig. 8 Deconvolution of the PL emission curves for the films: **a** Ti300, **b** Ti500, **c** Ti700, **d** In300, **e** In500, **f** In700, **g** TiIn300, **h** TiIn500 and **i** TiIn700

result of a combination of excited electrons and holes, the lower intensity indicates the decrease in the rate of recombination and, thus a higher photocatalytic activity [35]. According to Pontes [15], this property is associated with the structural disorder of the inorganic phase, the photoluminescent spectrum is more intense when the material is subjected to longer thermal treatments (the carbon is eliminated without crystallization). This is a strong indication that the disordered phase (amorphous phase) is responsible for photoluminescence [36]. As the calcination temperature increases, the order begins to increase in the medium and long range, so that the electron–hole transitions diminish, thus reducing the intensity of the photoluminescent signal and, as a consequence, a high photocatalytic activity. This can be observed comparing Figs. 7 and 10 that the samples, which present the best result of the photocatalysis, have the lowest photoluminescence intensity and the samples that have the highest photoluminescence intensity present a worse performance in methylene blue photocatalysis.

The Fig. 8 shows the emission decomposition of thin films TiO_2, In_2O_3 and TiO_2/In_2O_3. The PL spectra of the films were de-convoluted in green, blue, violet, yellow, red and orange emissions. Each color represents different types of electronic transitions and is linked to a specific structural arrangement. According to Huang et al. [37] the blue and green emission are attributed to the oxygen vacancies within the structure of the material. P. Wu et al. [38] have mentioned that photoluminescence emissions observed in the visible range may be caused by the recombination of carrier concentration that occurs between valence band and oxygen vacancies acting as donor levels. Table 4 presents the values found, indicating the contribution of each one to the emissions of the thin films.

Based on the emission spectra shown in Fig. 7 it is possible to calculate the chromaticity coordinates of the samples, as can be observed in Fig. 9. Most samples fall on blue region which are marked on CIE color coordinate diagram, which is important for the photocatalytic activities, since they are related to the presence of oxygen

Table 4 Contribution of the colors obtained with the decomposition of the PL curves

Sample	% Area						
	Violet	Blue	Cyano	Green	Yellow	Orange	Red
Ti 300	4.99	24.80	22.64	17.64	14.07	10.31	5.55
Ti 500	19.23	21.03	19.14	13.92	11.34	7.95	7.39
Ti 700	6.31	8.33	16.37	19.05	18.76	16.34	14.84
In 300	18.16	20.23	19.71	15.51	12.16	9.66	4.57
In 500	24.20	20.55	18.82	14.24	10.33	8.17	3.69
In 700	11.24	8.81	21.86	20.73	15.87	10.97	10.52
TiIn 300	11.88	13.02	16.15	17.09	15.19	13.59	13.08
TiIn 500	11.17	10.13	17.65	17.78	16.79	16.41	10.07
TiIn 700	11.71	19.76	37.57	22.93	8.03	-	-

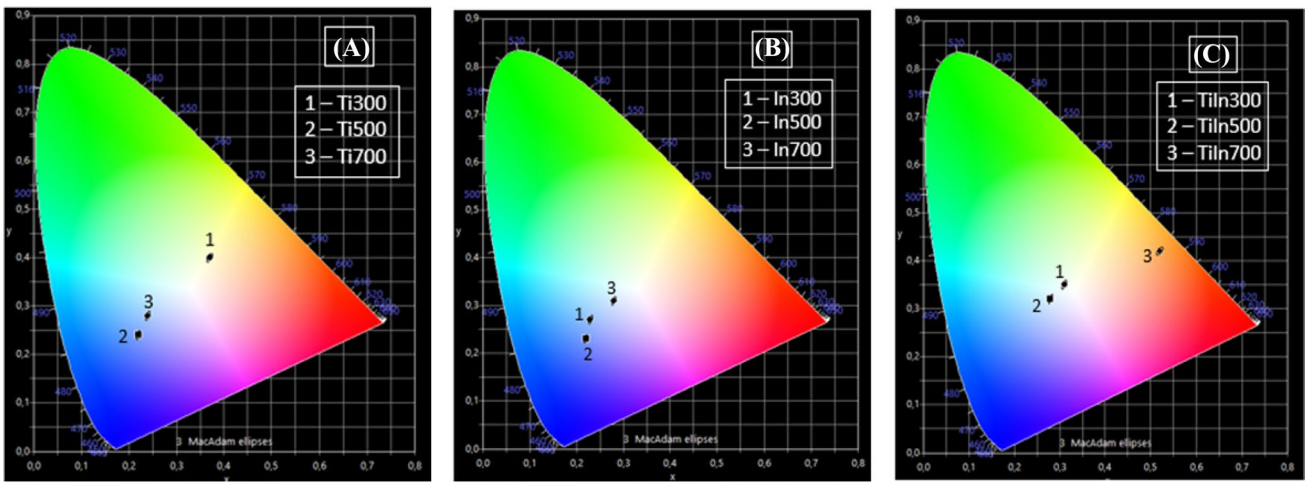

Fig. 9 Chromaticity coordinates for the samples of **a** TiO_2, **b** In_2O_3, **c** TiO_2/In_2O_3

waves, which can imprison electrons, thus avoiding the recombination of charges [39].

The relative values of the variation in the concentration of methylene blue were used to study the degradation of the TiO_2, In_2O_3, TiO_2/In_2O_3 thin films by UV radiation. The dye concentration as a function of the irradiation time is shown in Fig. 10 (I). During this process, it was observed that the concentration of methylene blue in the

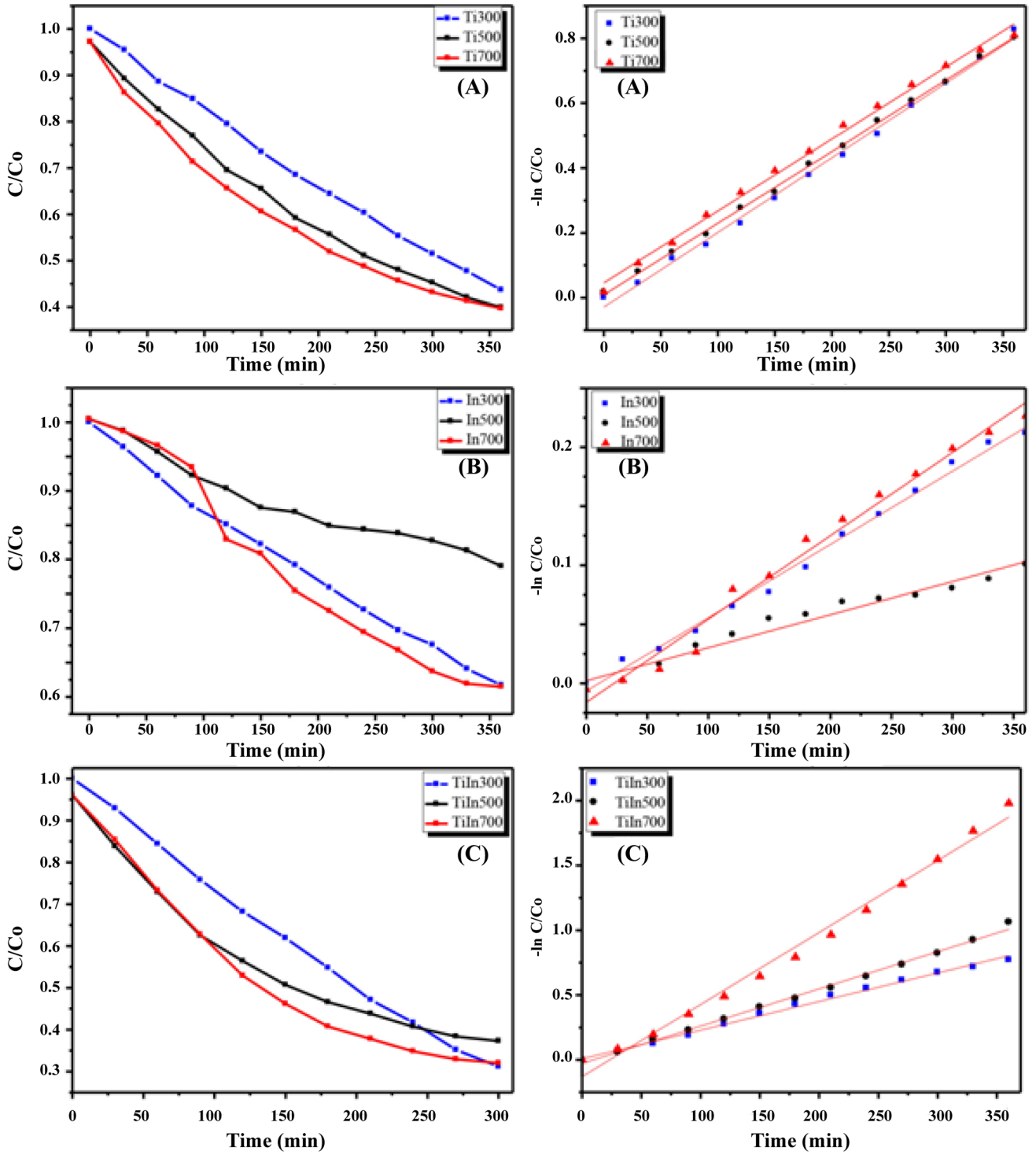

Fig. 10 Effect of crystallization temperature of the films **a** TiO_2, **b** In_2O_3 and **c** TiO_2/In_2O_3 with four layers under UV irradiation and photodegradation of methylene blue.

thin films decreases when they are exposed to UV radiation. According to Petronella [40], the engagement of the TiO_2 with In_2O_3 induces a significant increase in the photocatalytic activity than TiO_2 and In_2O_3. This significant increase is due to the positions of the conduction band (CB) and valence band (VB) of In_2O_3 and TiO_2. The In_2O_3 is able to transfer electrons from the conduction band of TiO_2.

Furthermore, the film of TiO_2/In_2O_3 calcined at 700 °C shows a slightly higher degradation rate than the film of TiO_2/In_2O_3 calcined from 300 to 500 °C, i.e., increasing the calcination temperature favors an in increase the photocatalytic activity. According to Zhou et al. [26], there is a significant increase in the photocatalytic activity SnO_2/TiO_2 composite with increasing calcination temperature.

Figure 10 (II) shows an image of the relative concentration of ln (C/C_0) relative to the irradiation time. Figure 11 also shows an image of the relative concentration of ln (C/C_0) relative to the irradiation time, but this time keeping the temperature constant. The behavior obtained experimentally, which is seen from the graphs, is a first order behavior of methylene blue in the degradation reaction. The reaction kinetics of dye MB were calculated using Eq. 3 [41].

$$\ln(C/C_0) = kt \tag{3}$$

where C_0 is the concentration before irradiation of MB and C is the concentration of MB after a certain irradiation time. The linear regression value obtained in this study was 0.99. According to Sanoop, for all experimental results by linear regression of ln data (C/C_0) versus irradiation time,the value of R2 is greater than 0.95 [41].

The recyclability of the samples TiO_2, In_2O_3 and TiO_2/In_2O_3 treated at 300, 500, and 700 °C were also investigated. The photocatalytic tests were performed using the same photocatalysts three times during each cycle of 350 min and the results are shown in Fig. 12.

The photocatalytic process has been widely used in the treatment of domestic and industrial wastewater and reuse of photocatalysts becomes very important, because it indicates, the ability of the material to remain active even after use. According to Fig. 12, it is possible to observe that that the photocatalyst retains its efficiency even when reused after three reaction cycles, it can be said that there is not a considerable loss of mass during washing. Cycling use as well as maintaining high photocatalytic activity are critical issues for long-term use in practical applications of the catalyst. Therefore, two criteria are required to be considered: (i) the stability of the catalyst to maintain its high activity over time, as shown in Fig. 12, and (ii) The ease with which the catalyst could be recycled from solution [42].

4 Conclusion

In this study, Multilayer TiO_2, In_2O_3 and TiO_2/In_2O_3 thin films were successfully synthesized using the Complex Polymerization Method (CPM) by varying the calcination temperature. The results indicated that the addition of In_2O_3 suppress the growth of TiO_2 grains, which can reduce the reflectivity of the surface, as well as shifts the optical absorption of TiO_2 to the visible region, increasing the photocatalytic activity of the films compared to pure TiO_2. The films were also recycled and reused for three cycles and showed to be efficient photocatalysts for degrading dyes, result quite satisfactory. The photoluminescence of these films is strongly influenced by the temperature of crystallization, an increase in temperature decreases the intensity of photoluminescence. As the photoluminescence signal is the result of a combination of excited electrons and holes, the lower intensity indicates the decrease in the rate of recombination and thus a higher the photocatalytic activity.

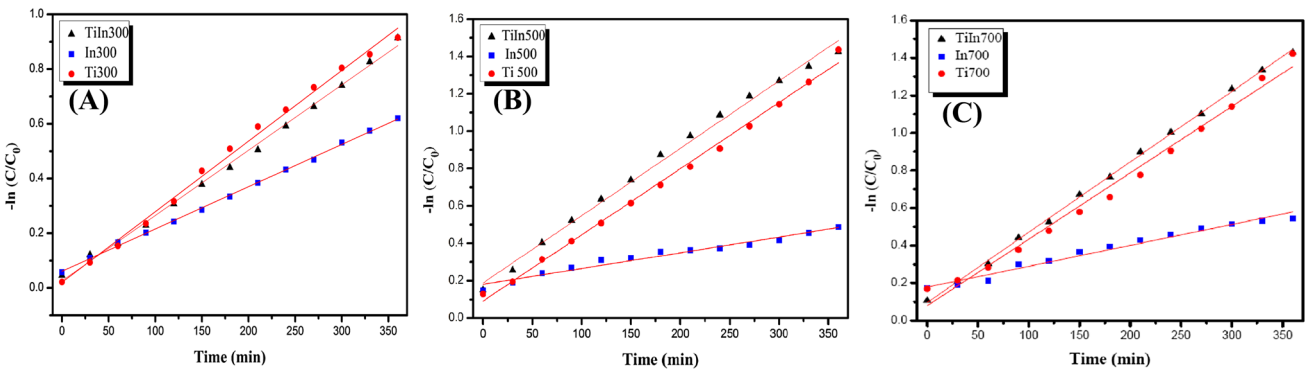

Fig. 11 Effect of the crystallization temperature of the films **a** TiO_2, **b** In_2O_3 and **c** TiO_2/In_2O_3 with four layers under UV irradiation and photodegradation of methylene blue, keeping the temperature constant

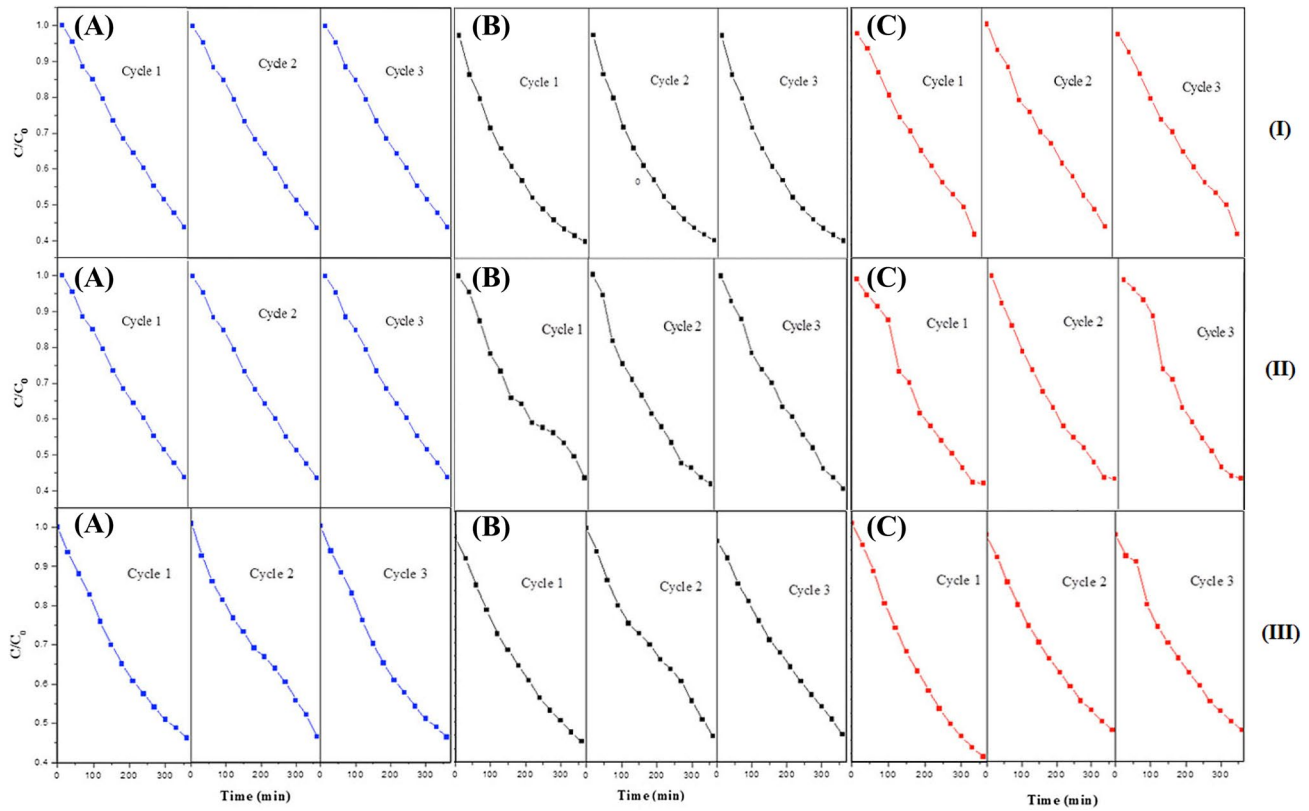

Fig. 12 Photocatalytic activity of the film (I) TiO_2, (II) In_2O_3 and (III) TiO_2/In_2O_3 in different crystallization temperatures for the degradation of methylene blue dye with three cycles used. **a** 300 °C, **b** 500 °C, **c** 700 °C

Acknowledgements The authors thank the financial support of the Brazilian research financing institutions: CAPES/PROCAD 2013/2998/2014, CNPq.

References

1. I. Stambolova, V. Blaskov, N. Kaneva, M. Shipochka, S. Vassilev, O. Dimitrov, A. Eliyas, Effect of post-synthesis acid activation of TiO_2 nanofilms on the photocatalytic efficiency under visible light. J. Phys. Conf. Ser. **558**, 012055 (2014)
2. S.A. Khayyat, R. Selvin, L.S. Roselin, A. Umar, Photocatalytic oxidation of phenolic pollutants and hydrophobic organic compounds in industrial wastewater using modified nonosize titanium silicate-1 thin film technology. J. Nanosci. Nanotechnol. **14**, 10–16 (2014)
3. S. Niyomkarn, T. Puangpetch, S. Chavadej, Mesoporous-assembled In_2O_3–TiO_2 mixed oxide photocatalysts for efficient degradation of azo dye contaminant in aqueous solution. Mater. Sci. Semicond. Process. **25**, 112–122 (2014)
4. L.G.J. De Haart, A.J. De Vries, G. Blasse, On the photoluminescence of semiconducting titanates applied in photoelectrochemical cells. Solid State Chem. **59**, 291 (1985)
5. T. Yasuda, K. Nishikawa, S. Furukawa, Structural colors from TiO2/SiO2 multilayer flakes prepared by sol–gel process. Dyes Pigm. **92**, 1122–1125 (2012)
6. A.R. Hernandez-Martinez, M. Estevez, S. Vargas, F. Quintanilla, R.J. Rodriguez, Natural pigment based dye sensitized solar cells. Appl. Res. Technol. **10**, 38–47 (2012)
7. A.A. Annenkova, M.V. Korzhikb, P. Lecoq, Lead tungstate scintillation material. Nucl. Instrum. Methods Phys. Res. Sect. A **490**, 30–50 (2002)
8. J. Kim, S. Do Hanb, H.D. Leea, J.S. Wanga, I. Singhc, S.V. Kornilov, Fabrication and characterization of humidity sensor based on (Li_2MoO_4) x $(CaMoO_4)1$ – x system. Mater. Sci. Eng. B. **116**, 226–230 (2005)
9. A. Apostolopoulou, D. Sygkridou, A. Rapsomanikis, A.N. Kalarakis, E. Stathatos, Enhanced performance of mesostructured perovskite solar cells in ambient conditions with a composite TiO_2–In_2O_3 electron transport layer. Solar Energy Mater. Solar Cells. **166**, 100–107 (2017)
10. Y. Chen, X. Zhou, X. Zhao, X. He, X. Gu, Crystallite structure, surface morphology and optical properties of In_2O_3–TiO_2 composite thin films by sol–gel method. Mater. Sci. Eng. B. **151**, 179–186 (2008)
11. C. Ramana, R. Vemuri, I. Fernandez, A. Campbell, Size-effects on the optical properties of zirconium oxide thin films. Appl. Phys. Lett. **95**, 231905 (1–3) (2009)
12. D. Tahir, S.K. Oh, H.J. Kang, S. Tougaard, Composition dependence of dielectric and optical properties of Hf-Zr-silicate thin films grown on Si (100) by atomic layer deposition. Thin Solid Films. **616**, 425–430 (2016)
13. A. Ortiz, J. Alonso, E. Haro-Poniatowski, Spray deposition and characterization of zirconium-oxide thin films. J. Electron. Mater. **34**, 150–155 (2005)

14. F.E. Ghodsi, F.Z. Tepehan, G.G. Tepehan, Electrochromic properties of heat-treated thin films of CeO_2–TiO_2–ZrO_2 prepared by sol–gel route. Sol. Energy Mater. Sol. Cells. **92**, 234–239 (2008)
15. F.M. Pontes, E. Longo, J.H.G. Rangel, M.I. Bernardi, E.R. Leite, J.A. Varela, Ba1-xSrxTiO$_3$ thin films by polymeric precursor method. Mater. Letter. **43**(5–6), 249 (2000)
16. M.B. Sarkar, A. Mondal, B. Choudhuri, B.K. Mahajan, S. Chakrabartty, C. Ngangbam, Enlarged broad band photodetection using Indium doped TiO_2 alloy thin Film. J. Alloy. Compd. **615**, 440–445 (2014)
17. W. Chen, C. Takai, H.R. Khosroshahi, M. Fuji, T. Shirai, SiO2/TiO2 double-shell hollow particles: fabrication and UV–Vis spectrum characterization. Adv. Powder Technol. **27**, 812–818 (2016)
18. A.K. Batra, A.K. Chilvery, P. Guggilla, M. Aggarwal, J.R. Currie micro- and nano-structured metal oxides based chemical sensors: an overview. J. Nanosci. Nanotechnol. **14**, 2065–2085 (2014)
19. Y. Zhang, J. Yu, K. Sun, Y. Zhu, Y. Bu, Z. Chen, Indium oxide thin film as potential photoanodes for corrosion protection of stainless steel under visible light. Mater. Res. Bull. **53**, 251–256 (2014)
20. A. Qurashi, J.A. Rather, T. Yamazakid, M. Sohail, K.D. Wael, B. Merzougui, A.S. Hakeem, Swift electrochemical detection of paraben an endocrinedisruptor by In_2O_3 nanobricks. Sens. Actuat. B. **221**, 167–171 (2015)
21. K. Hashimoto, H. Irie, A. Fujishima, TiO_2 photocatalysis: a historical overview and future prospects. Jpn J. Appl. Phys. **44**, 8269–8285 (2005)
22. B.M. Reddy, I. Ganesh, A. Khan, Preparation and characterization of In_2O_3-TiO_2 and V_2O_5/In_2O_3-TiO_2 composite oxides for catalytic applications. Appl. Catal. A. **248**, 169–180 (2003)
23. S.K. Poznyak, D.V. Talapin, A.I. Kul, Optical properties and charge transport in nanocrystalline TiO_2 –In_2O_3 composite films. Thin Solid Films. **405**, 35–41 (2002)
24. P. Scherrer, Determination of the size and internal structure of colloidal particles using X-rays, Nachr. Ges. Wiss. Göttingen. **26**, 98–100 (1918)
25. C. Li, T. Ming, J. Wang, J. Wang, J.C. Yu, S.Yu, Ultrasonic aerosol spray-assisted preparation of TiO2/In2O3 composite for visible-light-driven photocatalysis. J. Catal. **310**, 84–90 (2014)
26. M. Zhou, J. Yu, S. Liu, P. Zhai, L. Jiang, Effects of calcination temperatures on photocatalytic activity of SnO_2/TiO_2 composite films prepared by an EPD method. J. Hazard. Mater. **154**, 1141–1148 (2008)
27. P.F.S. Pereira, I.C. Nogueira, E. Longo, E.J. Nassar, I.L.V. Rosa, L.S. Cavalcante, Rietveld refinement and optical properties of SrWO4:Eu3 + powders prepared by the non-hydrolytic sol-gel method. J. Rare Earths. **33**, 113 (2015)
28. Y. Chen, X. Zhou, X. Zha, X. He, X. Gu, Crystallite structure, surface morphology and optical properties of In_2O_3–TiO_2 composite thin films by sol–gel method. Mater. Sci. Eng. B. **151**, 179–186 (2008)
29. K. Boubaker, A physical explanation to the controversial Urbach tailing universality. Eur. Phys. J. Plus. **126**, 1–4 (2011)
30. F. Urbach, The long-wavelength edge of photographic sensitivity and of the electronic absorption of solids. Phys. Rev. **92**, 1324 (1953)
31. S.S. Chiad, W.A. Jabbar, N.F. Habubi, Effects of annealing on the electronic transitions of ZnS thin films. J. Arkansas Acad. Sci., **65**, (2011)
32. H.S. Kim, H.G. Na, J.C. Yang, C. Lee, H.W. Kim, Synthesis, structure, photoluminescence, and raman spectrum of indium oxide nanowires. Acta Phys. Pol. A. **119**, 143–145 (2011)
33. R. Desai, S.K. Gupta, S. Mishra, P.K. JHA, A. Pratap, The synthesis of Tio2 nanoparticles by wet-chemical method and their photoluminescence, thermal and vibrational characterizations: effect of growth condition. Int. J. Nanosci. **10**, 1249–1256 (2011)
34. J. Jasieniak, J. Pacifico, R. Signorini, A. Chiasera, M. Ferrari, A. Martucci, P. Mulvaney, Luminescence and amplified stimulated emission in CdSe–ZnS-nanocrystal- doped TiO_2 and ZrO_2 waveguides. Adv. Funct. Mater. **17**, 1654–1662 (2007)
35. S. Husain, L.A. Alkhtaby, E. Giorgetti, A. Zoppi, M.M. Miranda, Investigation of the role of iron doping on the structural, optical and photoluminescence properties of sol–gel derived TiO_2 nanoparticles. J. Lumin. **172**, 258–263 (2016)
36. P.R. de Lucena, F.M. Pontes, C.D. Pinheiro, E. Longo, P.S. Pizani, S. A.G. L.ázaro, Souza, I. M. G. dos Santos (2004), Fotoluminescência em materiais com desordem estrutural. Cerâmica. **50** 314
37. Z. Huang, C. Chai, X. Tan, A. W., Yuan, Z., Zhou, Photoluminescence properties of the In_2O_3 octahedrons synthesized by carbothermal reduction method. Mater. Lett. **61**, 5137–5140 (2007)
38. P. Wu, Q. Li, C.X. Zhao, D.L. Zhang, L.F. Chi, T. Xiao, Appl. Surf. Sci. **255**, 3201e3204 (2008)
39. D.S. Dalavi, R.S. Devan, R.S. Patil, Y. Ma, P.S. Patil, Electrochromic performance of sol–gel deposited NiO thin film. Mater. Lett. **90**, 60–63 (2013)
40. F. Petronella, S. Rtimi, R. Comparelli, R. Sanjines, C. Pulgarin, M.L. Curri, J. Kiwi, Uniform TiO_2/In_2O_3surface films effective in bacterial inactivationunder visible light. J. Photochem. Photobiol. A. **279**, 1–7 (2014)
41. P.K. Sanoop, S. Anas, S. Ananthakumar, V. Gunasekar, R. Saravanan, V. Ponnusami, Synthesis of yttrium doped nanocrystalline ZnO and its photocatalytic activity in methylene blue degradation. Arab. J. Chem. **9**, S1618–S1626 (2016)
42. J. Sin, S. Lam, K. Lee, A. Mohamed, Preparation and photocatalytic properties of visible light-driven samarium-doped ZnO nanorods. Ceram. Int. **39**, 5833–5843 (2013)